

Effect of linear energy transfer (LET) on complexity of α -particle-induced chromosome aberrations in human CD34⁺ cells.

Rhona M. Anderson^{1,2}, David L. Stevens¹, Natalia D. Sumption¹, K. M. Stuart Townsend¹, Dudley T. Goodhead¹ and Mark A. Hill¹.

¹MRC Radiation and Genome Stability Unit, Harwell, Didcot. OXON. UK. OX11 0RD.

²Centre for Cell and Chromosome Biology, Division of Biosciences, Brunel University, West London. UB8 3PH.

Number of copies submitted = submitted online

Number of figures = 6

Number of tables = 3

Proposed running head = Human stem cells exposed to α -particles

Corresponding author = Rhona M. Anderson

Centre for Cell and Chromosome Biology

Division of Biosciences

Brunel University

West London UB8 3PH

Tel: +44 (0)1895 267138

Fax: +44 (0) 1895 274348

e-mail: rhona.anderson@brunel.ac.uk

Anderson, R.M, Stevens, D.L., Sumption, N.D., Townsend, K.M S., Goodhead, D.T. and Hill, M.A. Effect of linear energy transfer (LET) on complexity of α -particle-induced chromosome aberrations in human CD34⁺ cells. *Radiat. Res.*

The aim of this study was to assess the relative influence of linear energy transfer (LET) of α -particles on chromosome aberration complexity in the absence of significant other track structure differences. To do this we irradiated human haemopoietic stem cells (CD34⁺) with α -particles of various incident LET values (110 - 152 keV/ μ m, with mean LETs through the cell of 119 – 182 keV/ μ m) at an equi-fluence of approximately 1 α -particle/cell and assayed for chromosome aberrations by m-FISH. Based on a single harvest time to collect early division mitosis, complex aberrations were observed at comparable frequencies irrespective of incident LET, however when expressed as a proportion of the total exchanges detected, their occurrence was seen to increase with increasing LET. Cycle analysis to predict theoretical DNA double strand break rejoining cycles was also carried out on all complex chromosome aberrations detected. By doing this we found that the majority of complex aberrations are formed in single non-reducible cycles that involve just 2 or 3 different chromosomes and 3 or 4 different breaks. Each non-reducible cycle is suggested to represent ‘an area’ of finite size within the nucleus where double strand break repair occurs. We suggest that local density of damage induced and proximity of independent repair areas within the interphase nucleus determine the complexity of aberration resolved in metaphase. Overall, the most likely outcome of a single nuclear traversal of a single α -particle in CD34⁺ cells is a single chromosome aberration per damaged cell. As the incident LET of the α -particle increases, the likelihood of this aberration being classed as complex is greater.

INTRODUCTION

In essentially all practical environmental and therapeutic exposures to α -particles, cells are exposed to a range of α -particle energies and therefore linear energy transfer (LETs) as the α -particles slow down and stop within the irradiated tissue. While most experiments on the effects of α -particles have been carried out at a single LET, studies presented in this paper investigate the effect of α -particle traversals over a range of LETs similar to those encountered within the tissue of a person exposed to α -particles from an internal radionuclide.

Ionisation events occur along the whole length of the α -particle track (ranges up to $\sim 70 \mu\text{m}$ from a ^{214}Po 7.7 MeV α -particle) which can deliver a large dose to a traversed cell (up to ~ 90 cGy, for a spherical cell of $8 \mu\text{m}$ diameter). As the α -particle loses energy and slows down, the average ionisation density per unit track length, specified by the LET, increases from $\sim 70\text{-}90 \text{ keV } \mu\text{m}^{-1}$ (depending on initial energy) to $\sim 220 \text{ keV } \mu\text{m}^{-1}$ at the Bragg peak close to the end of its range, beyond which, the LET quickly falls as the α -particle comes to a rest. Therefore the majority of cells will be traversed by α -particles with LETs of $\sim 100 \text{ keV } \mu\text{m}^{-1}$, but with a smaller number traversed at significantly higher LETs at the end of its track. The average number of DNA double strand breaks (dsb) induced by each traversal will increase with the mean LET of the particle through the cell nucleus and the proportion of complex dsb (dsb with additional strand breaks within 10 base pairs) is also expected to increase slightly, together with the degree of complexity of these breaks with additional associated base damages and strand breaks. Further, due to the short range of the δ -electrons (typically maximum range $< 0.1 \mu\text{m}$, with $\sim 90\%$ of

energy deposition within 10nm) , a single α -particle track will deposit a significant amount of energy along a narrow track resulting in a very non-homogeneous distribution of correlated damage through a nucleus, traversing only a limited number of chromosome territories.

Radon with its α -particle emitting progeny is the dominant source of environmental radiation exposure, with the majority of the exposure to the lung resulting from the intermediate decay products that become attached to natural aerosol particles that adhere to the lining of the lungs and airways when inhaled. Additionally, radon gas can be absorbed into the bloodstream and transported to various organs which can result in exposure of a range of cells, including the peripheral blood lymphocytes and haemopoietic stem cells . Similarly significant exposure may result from other internalised α -particle emitting nuclides. For low doses typically associated with human exposures, cells are either unirradiated or receive a single α -particle traversal separated in time by months or years with the proportion of unirradiated to irradiated cells increasing with decreasing dose. The energy deposited to the traversed cells by these isolated α -particles, is independent of dose at these low exposures. The effect of single α -particle traversals is therefore important in understanding the mechanisms of radiation action and the risk associated with low dose exposures.

It is well established that the proportion of chromosome exchanges classified as complex (3 or more breaks in 2 or more chromosomes) increases with increasing dose in the low-linear energy transfer (LET) range, such as X-rays or γ -rays , but *largely* independent of dose when the LET is >100 keV/ μm . For a number of different particles, as the LET increases from ~ 100 - >1000 keV/ μm , the frequency and complexity of

complex aberration induced also increases compared to that observed for low-LET radiation. Aberration complexity is not dictated by LET alone however, but also by the qualitative structure of the radiation track at a given LET and the proportion or volume of the cell irradiated. Therefore two different particles of the same LET result in differences in the yields and complexity of aberrations observed. So at low doses, where irradiated cells will only be traversed by a single particle, the LET and track structure, (on a DNA, chromatin and cell-wide basis) will determine the type of aberration ultimately resolved.

In a previous study, the effect of irradiating human peripheral blood lymphocytes (PBL) with α -particles of LET 121 keV/ μm was examined. The main conclusion was that the traversal of a single α -particle through a single PBL cell nucleus predominantly results in the induction of a single complex chromosome exchange. A possible mechanism of how such α -particle-induced 'complexes' may be formed was also proposed. To address whether complex exchanges are a constant feature of α -particle exposure of spherical cells, irrespective of which segment of the track actually traverses the cell nucleus, the effect of irradiating human CD34⁺ cells with α -particles of various LETs, is examined. CD34⁺ cells are spherical in shape, hierarchical to mature PBL, capable of self-renewal and may have leukaemogenic relevance. From the natural environment, bone marrow is exposed *in vivo* to α -emitting radionuclides, including radon and its progeny due to the high solubility of radon gas in fat cells such as those found in the bone marrow, . Hence some CD34⁺ cells are directly exposed *in vivo*. The overall focus of this study is to examine the influence of LET, in the absence of other differences in track structure, at least at the cellular level, on the complexity of α -particle-induced aberrations.

MATERIALS AND METHODS

Cell Culture

Frozen human bone marrow CD34⁺ cells were obtained commercially (Poietics, Cambrex, UK and AllCells, LLC, USA) in vials of 1x10⁶ cells (Samples are anonymised and exempt from Ethical Review Procedures). When required, individual vials were removed from liquid nitrogen and thawed quickly by immersing in a 37°C water bath. Once thawed, the cells were diluted with 5 ml of pre-warmed basic media (StemSpan™ (Stemcell Technologies, SARL, UK) containing 100 IU/ml penicillin, 100µg/ml streptomycin and 21 U DNase (Type II-S, Sigma, UK)) by slowly adding the cells to the medium in a drop-wise fashion. The cells were left to settle then centrifuged at 200g for 12 minutes, resuspended in 33 µl of basic medium, plated onto a Hostaphan (0.35 mg cm⁻² polyethylene terephthalate; Hoechst) based dish (11 µl/dish) and spread using a CR39 disc (28.4 mm diameter) to form a monolayer for sham or α-particle irradiation. Confocal microscope measurements were used to confirm that cells were in contact with the Hostaphan base at the time of irradiation. Additionally, etching (40% solution of potassium hydroxide at 60°C for ~ 60 min) of the CR-39 discs was performed following irradiation to view the resultant α-particle induced pits and confirm good transmission of the α-particles across the irradiated sample.

After irradiation, the cells were washed from the Hostaphan dishes by rinsing directly with the final volume of culture medium (basic media with 50ng/ml SCF,

50ng/ml Flt-3, 10ng/ml IL-3, 10ng/ml IL-6, 10ng/ml GM-CSF (R&D Systems, UK), 10µg/ml 5'-bromodeoxyuridine (BrdU) (Sigma), 100U/ml penicillin and 100µg/ml streptomycin) to give a seeding density of $0.5 - 1.0 \times 10^5$ /ml. The cells were then incubated at 37°C in 95% air/5% CO₂ in T25 flasks in an upright position for 49 hr. CD34⁺ cells were harvested to obtain early division mitoses by the addition of 0.05µg/ml demecolchicine (Sigma) for the last 6 hr of culture. The cells were centrifuged at 200g for 12 min, resuspended in 5 ml hypotonic solution (1:1 0.075M potassium chloride : 0.8% sodium citrate; 8 min at 37°C), centrifuged once more and fixed in ice-cold 3:1 methanol:glacial acetic acid (v:v, BDH). The cell suspension was stored at -20°C. Fractions of cells from the same sample were assayed separately for chromosome aberrations (m-FISH) and cell cycle status (Harlequin staining).

α-Particle Irradiation

Cells were exposed to an essentially mono-energetic, parallel source of α-particles using the Medical Research Council (MRC) ²³⁸Pu α-particle irradiator previously described . The irradiator was designed so that the energy and therefore the LET of the incident α-particles can be varied, by varying the height of the ²³⁸Pu source relative to the exit window of the helium filled chamber. The energy of the α-particles for the various source height settings were obtained using a surface barrier detector and the related absorbed dose rate calculated from flux measurements made using plastic CR-39 track detectors and allowing for subsequent decay in the activity with time ($t_{1/2} = 87.7$ years).

For this study, three different α -particle energies were chosen to simulate track segments through the cells covering almost the whole length of the α -particle track from 3.82 MeV downwards, assuming a cell monolayer depth of 7-8 μm up to $\sim 220 \text{ keV}/\mu\text{m}$ close to the Bragg peak (Fig. 1). The α -particle energies on the incident surface of the cell monolayer were either 3.82, 3.26 or 2.23 MeV corresponding to incident LETs of 110, 121 and 152 $\text{keV}/\mu\text{m}$, rising to maximum values of 131, 153 and 220 $\text{keV}/\mu\text{m}$. Details of the α -particle exposure parameters are given in Table 1.

Convenient exposure times were calculated to deliver an average fluence of ~ 1 α -particle/cell for each LET, based on cells of 7 μm diameter, similar to the dimensions of PBL cells .

Multiplex FISH (m-FISH)

Fresh slides of metaphase cells were hardened and pretreated with RNase A (100 $\mu\text{g}/\text{ml}$ in 2xSSC) and pepsin ($1:20 \times 10^3$ in 10 mM HCL) as described previously . For hybridisation, cells were denatured in 70% formamide/2xSSC at 72°C for 3 min and dehydrated for 1 min each in 70/90/100% ethanol. In parallel, an aliquot of SpectraVision™ Assay (Vysis, UK) 24-colour paint cocktail was denatured at 73°C for 6 min. Probe was then applied to slides, which were left to hybridise for 36-48 h at 37°C before being washed in 0.4xSSC/0.3% Igepal (Sigma, UK) at 71°C for 2-3 min and in 2xSSC/0.1% Igepal at room temperature for 10 sec. Cells were counterstained using DAPI III (Vysis, UK), sealed and stored in the dark at -20°C.

Chromosome aberrations were analysed as previously described . In brief, metaphase chromosomes were visualised using a 6-position Olympus BX51 fluorescent

microscope containing individual filter sets for each component fluor of the SpectraVision (Vysis (UK) Ltd) probe cocktail plus DAPI. Digital images were captured for m-FISH using a charged-coupled device (CCD) camera (Photometrics Sensys CCD) coupled to and driven by Genus (Applied Imaging, UK). In the first instance, cells were karyotyped and analysed by enhanced DAPI banding. Detailed paint analysis was then performed by assessing paint coverage for each individual fluor down the length of each individual chromosome, using both the raw and processed images for each fluor channel. A cell was classified as being apparently normal if all 46 chromosomes were observed by this process, and subsequently confirmed by the Genus m-FISH assignment, to have their appropriate combinatorial paint composition down their entire length.

Abnormalities were identified as colour-junctions down the length of individual chromosomes and/or by the presence of chromosome fragments. The paint composition was used to identify the chromosomes involved. No attempt was made to consider intra-chromosomal events such as inversions in this assessment. Each exchange aberration involving 3 or more breaks in 2 or more chromosomes was classed as Complex and assigned the most conservative C/A/B (minimum number of Chromosomes/Arms/Breaks involved) , while exchange aberrations involving a maximum of two breaks in two chromosomes were classified as Simple. Chromosome breaks not involving additional chromosomes were classed as Break-only.

'Cycle' analysis

Predictions as to the relative physical nuclear relationship between multiple damaged chromatin 'ends' at time of misrepair can be made by analysing m-FISH data

using a theoretical methodology termed as ‘cycle’ analysis . Broadly speaking, this analysis deconstructs the ‘observed’ aberration in metaphase to make predictions as to how it could have been formed in interphase (for detail see). Accordingly, complex aberrations that were formed through the illegitimate repair of damaged chromatin in the same intranuclear space can be distinguished from those complex aberrations that were formed in two (or more) spatially separated, but sequentially linked, intranuclear repair sites. For classification purposes a ‘cycle’ is defined as the completion of the illegitimate repair of both ends of a chromosome break . Thus, a complex is classified as non-reducible (NR) of size n if all of the free-ends of all of the breaks misrepair to produce the complex observed by m-FISH in one cycle. n denotes the actual number of breaks in the cycle (expressed as cn , for example $c3$). A sequential exchange complex (SEC) defines those complexes that could theoretically be formed in multiple smaller cycles of exchange, but where independent cycles are linked by the involvement of common chromosomes .

To characterise each complex exchange, using cycle analysis, as forming via either NR or SEC mechanisms, complex aberrations were analysed as previously described . Briefly, two diagrams were drawn for each aberration using coloured markers, one representing the damaged chromosomes as seen in the m-FISH karyotype and the second, the participating ‘normal’ chromosomes with relative positions of chromosome breakpoints superimposed. Each break was then sequentially numbered so that each free-end of each break was uniquely identified. Starting at free-end #1, each numbered ‘end’ was then paired with its illegitimate partner, based on the m-FISH pattern, until free-end #2 becomes closed. This defines one cycle of size n . When the complex exchange was

not of the NR type and breaks remained unpaired i.e. if a SEC, then the above process was repeated until all 'free-ends' were illegitimately complete. Each complex exchange was then assigned into one of three groups: those that could only be formed as a non-reducible (NR) cycle, those that could be formed as either a NR cycle or as a sequential exchange (SEC) (NR+SEC), and those that could only be formed as a SEC. For many complex aberrations, a number of 'rejoining cycles' were theoretically capable of reconstructing the observed complex. All possibilities were derived, but to standardise the data, only the most conservative, or obligate cycle structure, was employed for mechanistic interpretations .

Harlequin staining

Metaphase cells were determined to be in either the 1st, 2nd or 3rd cell division after stimulation *in vitro* based on their Harlequin staining pattern . Slides of metaphase cells were prepared as described above and left in the dark at room temperature to 'age' for between 3-5 days. The slides were then immersed in Hoechst 33258 (Sigma, UK) (~20 µg/ml in distilled water) for 10 min before being transferred to a flat tray and submerged (~1 mm depth) face up in 2xSSC and exposed to light from mercury vapour lamp (Phillips TYP. 57135 G) for 25 min. After this time, the slides were removed and washed three times in distilled water for 5 min each, air-dried and finally stained with 6% Giemsa for 5 min.

Detection of apoptotic CD34⁺ cells

CD34⁺ cells were thawed, washed and prepared as a pellet for irradiation as described above. After either sham or α -particle irradiation, cells were seeded in 24-well plates at a density of $\sim 1 \times 10^5$ /ml in a total volume of 1 ml culture media. Sham-irradiated wells were either not treated (negative control) or treated with actinomycin-D (5 μ M in 2.5% DMSO) (positive control) from the time of stimulation in culture medium and incubated for the appropriate length of time (24, 49, 73 or 97 hr) in 95% air/5% CO₂.

The RAPID Annexin V binding assay kit (Oncogene) was used throughout. After the appropriate length of time, cells were gently resuspended and transferred into eppendorf tubes. 10 μ l of media binding reagent was added to each tube and 1.25 μ l of Annexin V-FITC added to all tests and appropriate control tubes. The reagents were gently distributed through the cell suspension and left to incubate in the dark at room temperature for 15 min. Cells were then pelleted by centrifugation at 1000g for 5 min and the supernatant removed. After resuspension in 0.5 ml of 1x binding buffer, the cells were transported on ice (in the dark) for immediate FACS (fluorescence-activated cell sorter) analysis (Becton Dickinson, UK). 10 μ l of propidium iodide (PI) was added to all test samples and appropriate controls just prior to analysis.

Positive and negative control samples were analysed in parallel to each test sample. Background auto-fluorescence was accounted for and discrimination between Annexin V-FITC (A⁺) and PI (P⁺) signal was confirmed using positive control samples of A⁺/P⁻ and A⁻/P⁺. Determination of the apoptotic cell quadrant from the dead cell quadrant was achieved using the positive control A⁺/P⁻ plot. Values for control samples remained

essentially constant between experiments, allowing experiments to be pooled for further analysis.

Statistical analysis

Tests are Fisher's exact test and the conditional binomial test. p-values are 1-tailed in the case of sham versus irradiated and 2-tailed for irradiated versus irradiated. 95% statistical significance used throughout.

RESULTS

Induction of chromosome aberrations

The total number of CD34⁺ cells analysed and chromosome aberrations detected by m-FISH 49 hr after exposure to either sham or α -particle irradiation of various LET are shown in Table 2. For sham-irradiated CD34⁺ cells, the frequency of damaged cells is significantly lower than that observed for each of the α -particle irradiated populations ($p < 0.000001$), while the frequency of exchanges (< 0.005) and breaks (0.01) are in keeping with expected background levels for PBL .

Complex chromosome aberrations are induced in CD34⁺ cells after exposure to a mean of ~ 1 α -particle/cell, at comparable frequencies, irrespective of incident LET (0.183, 0.152 and 0.205 for 110, 121 and 152 keV/ μ m respectively, $p > 0.20$ for all) (Table 2). The average size of each complex detected by m-FISH involves ~ 3 different

chromosomes and ~5 different breaks (complexes range from involving 2 different chromosomes and 3 breaks to 8 chromosomes and 12 breaks) (Table 3). A significant increase in the frequency of simple exchanges induced in CD34⁺ cells was observed however after exposure to α -particles of 110 keV/ μ m (0.230) compared to 121 keV/ μ m (0.129) ($p=0.016$) and 152 keV/ μ m (0.094) ($p=0.00024$) (Table 2). Thus, the proportion of exchanges classified as complex increases after exposure to α -particles of increasing LET (statistical significance only reached between 110 keV/ μ m and 152 keV/ μ m ($p=0.0027$)) (Table 2).

To assess whether the LET difference in total exchange frequency reflected differences in the spectrum of aberration complexity within each damaged cell, data were expressed according to whether each damaged cell contained at least one simple or at least one complex exchange (Figure 2). In addition, the distribution of cells that contained single or multiple exchanges was plotted (Figure 3). Accordingly, the increased frequency of simple exchanges observed after exposure to 110 keV/ μ m ($p=0.037$) or 121 keV/ μ m ($p=0.0033$) in comparison to 152 keV/ μ m, was found to be a consequence of more damaged cells containing simple-type exchanges only (Figure 2). Thus, exposure of CD34⁺ cells to a mean of ~1 α -particle/cell of LET 110 or 121 keV/ μ m only results in the induction of a complex exchange in ~ 40-50% of damaged cells, in contrast to that seen after exposure of 152 keV/ μ m (~ 80%) (Figure 2). In terms of spectrum of exchange per damaged cell, slightly more cells contained multiple simple exchanges after exposure to 110 keV/ μ m and slightly more cells contained multiple complex exchanges after 152 keV/ μ m, relative to each other (Figure 3).

Poisson distribution of α -particle nuclear traversals

The number of independent damage events observed by m-FISH in each damaged cell was compared with the number of α -particle tracks expected to traverse the cell nucleus. To accurately calculate the Poisson distribution of particle ‘hits’ according to nuclear area, the actual distribution of CD34⁺ cell sizes measured by confocal analysis and weighted for their likelihood of occurrence, was used (data not shown). Nuclear area was assumed to be 0.67 of the cell area based on previous PBL measurements . Figure 4 shows the association between the fraction of the traversed nuclei which were traversed by 1, 2, 3 or 4 α -particles with the fractions of damaged cells classified with 1, 2, 3 or 4 independent events, for each LET exposure. The associations for all LET exposures are remarkably close. Accordingly, it is unlikely that damage induced by δ -rays from α -particles traversing outside the nucleus contributed appreciably to the observed chromosomal damage, since the range of δ -rays emitted with maximum energy is $< 0.1 \mu\text{m}$ (Table 1). Another explanation is therefore required for the increased frequency of simple exchanges (see Discussion).

Theoretical cycle analysis of α -particle-induced complex chromosome exchanges

All possible 'rejoining cycles' of each visible complex exchange were derived as described in Methods and used to predict the physical relationship of damaged chromatin 'ends' relative to each other in the nucleus at the time of misrepair. To minimise ambiguity, only those complex aberrations that were observed in cells where no homologous pair was damaged were used. There are three groups of classification for cycle analysis: non-reducible (NR) cycle only, NR or sequential exchange complex (SEC) (NR+SEC) and SEC only .

80% of complex chromosome aberrations induced after exposure to α -particles of LET 110 keV/ μ m could, theoretically, only be formed as a single NR cycle. The size of each NR cycle ranged from c3-c9 (c3:c4:c5:c6:c9) in percentile proportions of 45:25:20:5:5 respectively and the number of different chromosomes involved, ranged from 2-7 (2:3:4:7) in proportions of 25:50:20:5. Thus, the majority of complex aberrations that are formed in single NR cycles involve just 2 or 3 different chromosomes and 3 or 4 different breaks. Similarly, 62% of the complex aberrations induced after exposure to α -particles of LET 121 keV/ μ m could only be formed as single NR cycles. The cycle size ranges from c3-c6, with c3 being the most common, accounting for 69% of all NR cycles. The number of different chromosomes involved in each NR cycle ranged from 2-5, with the smaller number (2 or 3 chromosomes) comprising ~80% of the total. Of the complex aberrations induced after exposure to α -particles of LET 152 keV/ μ m, 72% could be derived as being formed only as single NR cycles. Cycle sizes ranged from c3-c7, with a cycle order of c3 (58%) and 2-3 different chromosomes (~88% all NR complexes) (chromosome range 2-5) representing the most common. Thus, large misrepair cycles involving more than 3 different chromosomes and 4 different breaks

were rare events for all LET exposures in CD34⁺ cells. No statistical difference was observed in the proportion of complex exchanges that could theoretically be formed only as single NR cycles, between the different LET exposures ($p=0.40$).

20%, 38% and 28% of complex aberrations induced after exposure to α -particles of LET 110, 121 and 152 keV/ μm in CD34⁺ cells respectively, could, theoretically, be formed either as a single NR cycle or by SEC mechanisms (NR+SEC) (data not shown). The most common cycle size was c2 in all cases (accounting for ~50% of all) and cycle sizes greater than c4 occurred rarely for all LET exposures. The number of different chromosomes involved in each complex ranged from 2-7 for all LET exposures, however similar to the NR-only group, those involving more than 4 different chromosomes occur rarely. No complex aberrations were observed which could be formed by SEC mechanisms alone.

Effect of LET on CD34⁺ cell cycle progression

To assess the effect of various LET on CD34⁺ cell cycle progression, cells were stained using the Harlequin technique and determined to be in their 1st, 2nd or 3rd cell division after irradiation. Overall, ~500 cells were scored for each exposure (110, 121 or 152 keV/ μm) at the sample times of 49 and 73 hr. Figure 5 shows the proportion of cells in each cell division at each time point. A pooled heterogeneity factor was used to test for differences and approximate standard errors calculated from this. These errors were used to compare the overall trend of cycling population between each exposure.

A similar proportion of cells were seen to be in their 1st and 2nd cell division after exposure to α -particles of LET 110 keV/ μ m, as observed for the sham irradiated population by 49 hr (Figure 5 a and b). This is different to that observed after exposure to α -particles of either LET 121 or 152 keV/ μ m, which both appear to be more delayed by comparison (Figure 5 c and d). By 73 hr, the trend looks similar for all irradiated populations with a suggestion of increased cell cycle delay in comparison to sham (Figure 5 a-d). The above trends were not associated with any detectable differences in mitotic index (a measure of the proportion of cells in metaphase) after 49 hr in culture, between sham or irradiated ($p>0.20$) or between LET exposures by 49 hr ($p=0.24$) or 73 hr ($p=0.95$) (data not shown). However, marginally fewer cells were in metaphase by 73 hr in populations exposed to 110 keV/ μ m ($p=0.043$) and 152 keV/ μ m ($p=0.048$), but not 121 keV/ μ m ($p=0.12$) compared to sham (data not shown).

Effect of LET on induction of apoptosis

To assess whether differing populations of CD34⁺ cells were induced to apoptose as a direct consequence of different LET exposure, the proportion of Annexin V positive stained cells was measured by flow cytometry at various times after exposure.

A significantly higher % of CD34⁺ cells were identified as apoptotic after treatment with actinomycin-D (5 μ M in 2.5% DMSO) (positive control) compared to the untreated negative control (mean of 29% compared to 13%, $p<0.000001$) (Figure 6). For CD34⁺ cells exposed to α -particle radiation for all LET exposures, the percentage of apoptotic cells observed was significantly greater relative to the negative control, for all

LET exposures ($p=0.00036$ at 24 hr, $p=0.019$ at 49 hr and $p=<0.00001$ for 73 hr). Considering the effect of LET on the induction of apoptosis, the only difference observed was between cells exposed to α -particles of LET 110 keV/ μm compared to 121 and 152 keV/ μm . Marginally fewer cells were identified as apoptotic after 24 hr in culture at the lower LET ($p=0.083$) (Figure 6).

DISCUSSION

Overall, comparable frequencies of complex aberrations were observed 49 hr after exposure to α -particles irrespective of incident LET studied (Table 2). Further, the complexity of each complex, in terms of number of different chromosomes and breaks visualised by m-FISH, was statistically similar for each LET exposure and in keeping with that previously observed for PBL. Thus, based on frequency or type of complex aberration alone, no significant difference in aberration complexity was observed after exposure to α -particles with incident LETs in the range 110 - 152 keV/ μm (mean LETs 119 – 182 keV/ μm). What this initially suggests, is that complex aberration formation is independent of dsb density within the range studied and that α -particle-induced clustered damage is of sufficient frequency and complexity, irrespective of incident LET, to result in the formation of complex chromosome aberrations. However, complex aberrations were not formed independent of LET. When expressed as proportions of the total exchanges induced, a decreased percentage of complex aberrations correlated with a decrease in incident LET, due to more simple exchanges being induced at the lower LET (Table 2). This elevated simple frequency corresponded with an increase in the

proportion of cells that contained just simple-type damage and also with an increasing, but not statistically significant, trend in percentage of damaged cells observed. Overall, this demonstrates that α -particles of lower incident LET do have a higher likelihood of inducing aberrations of lower complexity compared to α -particles of higher incident LETs (Figs. 2 and 3).

Cell cycle delay is known to be positively correlated with dose and LET in human lymphocytes . In addition, it has been shown elsewhere that the delay of cells containing complex aberrations increases as the LET increases, with the consequence that complex frequency (but not simple) will be influenced by collection time . Thus, the apparent independence in complex frequency observed in this study between incident LET exposures is likely to be a consequence of sampling since the data were generated from only one harvest time (49 hr after exposure). The relative difference in cell cycle delay and the proportion of cells induced to apoptose at various time points after exposure to α -particles of various incident LETs is shown in Figs. 5 and 6. From this it is suggested, that as a population, CD34⁺ cells exposed to α -particles of LET 110 keV/ μ m are delayed and, induced to apoptose within 24 hours, to a lesser degree, than those exposed to either 121 or 152 keV/ μ m (Figs. 5 and 6). Overall therefore, it is likely these comparative reductions in cell cycle delay and interphase cell death do correlate with a reduced complexity of chromosome aberration initially induced. However, the possibility cannot be excluded that the increased frequency of simples seen after exposure to 110 keV/ μ m is also contributed by, at least in part, damaged cells in their 2nd cell division after irradiation.

In this study, α -particle irradiations were carried out using a broad-beam irradiator, with the number of α -particle traversals Poissonly distributed, meaning that a proportion of the cells would be exposed to >1 α -particle. Thus, slightly more cells would be expected to have multiple simple exchanges after exposure to α -particles of LET 110 keV/ μ m and slightly more cells would be expected to have multiple complex aberrations after exposure to α -particles of LET 152 keV/ μ m than if each cell was traversed by just a single α -particle. This is consistent with observations and the prediction that each aberration is the product of the nuclear traversal of a single α -particle track (Figs. 3 and 4) .

In a previous study we analysed α -particle-induced aberrations in PBL and related aberration complexity with the number of different chromosome territories intersected by the α -particle track and the geometry of the cell irradiated . In addition, we predicted that as the number of territories intersected increased, then the likelihood that the complex aberration was formed via the sequential linking of smaller discrete exchange events, also increased . In terms of damaged chromatin dynamics therefore, this mechanism of complex formation infers a ‘limited migration’ of damaged chromatin within a particular ‘area’ for repair. Based on the theoretical cycle classification system used in this study, each ‘area’ translates to a single NR cycle . If valid, then the complexity of each aberration observed in metaphase is a consequence of the number of different chromatin ‘ends’ in each repair ‘cycle’ and also, the distribution of individual ‘cycles’ through neighbouring territories. For this latter point it is plausible to speculate that if less energy is deposited along the α -particle track through the nucleus, then the resulting damage would be expected to be more spatially separated than if the converse was the case. So at

lower incident LET, assuming only ‘limited migration’ of damaged chromatin can occur, this may lead to a reduction in the likelihood that the subsequent repair events could sequentially link to form SECs.

20%, 38% and 28% of the complex aberrations induced by α -particles of LET 110, 121 and 152 keV/ μ m respectively, were recorded as being in the NR+SEC group (i.e both mechanisms are theoretically possible). No statistically significant difference between the varying incident LET exposures was detected. However, the confidence with which SEC mechanisms could be assigned as a potential route of complex formation appeared to decrease with LET (data not shown). Consequently, a higher proportion of complexes are more likely to be formed in CD34⁺ cells in one single NR cycle after exposure to α -particles of lower LET.

The average dose and therefore the yield of dsb induced by each α -particle traversal will be higher for 152 keV/ μ m compared to 110 and 121 keV/ μ m (Table 1). Further, as the mean LET is increased through the nucleus, the density of clustered DNA damages also increases, meaning that an increased proportion of clustered damages could be induced within short distances of each other. Theoretically at least, chromatin ends from multiple, closely spaced clustered damage could associate for misrepair and form NR cycles of an increased size. Consequently when cycles of the order c2, representing simples, were included in the NR cycle size proportions, an increased trend with increasing LET was seen. Specifically, cycles of size c2:c3:c4:c5>c5 theoretically occurred in proportions of 71:13:7:7:2, 68:23:5:2:2 and 48:30:14:6:2 for 110, 121 and 152 keV/ μ m respectively. In other words, slightly more chromatin ends participate in each cycle after exposure to α -particles of higher LET compared to lower LET. Since on

average, each cycle involves just 2-3 different chromosomes, what this reflects is an increase in number of breaks per chromosome territory at higher LET .

Thus at a physical level, each NR cycle represents an area within the nucleus where repair of damaged chromatin takes place and the complexity of aberration ultimately resolved is dependent on the amount of damage in that 'local' area. Consequently, it is thought unlikely that damage repaired as a complex chromosome aberration will have been processed in a different 'type' of repair site to that which resulted in the formation of a simple exchange. Instead, the same mechanism for the misrepair of both types of exchange is expected such that aberration complexity is a consequence of the density of localised induced damage, coupled with the chance of each individual site linking via SEC mechanisms. This expectation is essentially independent of assumptions as to whether chromosome exchanges take place exclusively between radiation-induced breaks or whether 'undamaged' DNA can also be involved .

In conclusion, according to these findings, the most likely outcome of a single nuclear traversal of a single α -particle in CD34⁺ cells is a single chromosome aberration per damaged cell. As the incident LET of the α -particle increases, the likelihood of this aberration being classed as complex is greater. It is suggested that local density of damage induced and proximity of independent repair sites within the interphase nucleus determine the complexity of aberration resolved in metaphase. The relevance that simple exchanges can be directly induced in CD34⁺ cells for *in vivo* exposures to natural α -particle radiation will be discussed elsewhere (manuscript in preparation).

ACKNOWLEDGEMENTS

The authors are grateful to David Papworth (now retired from the MRC Radiation and Genome Stability Unit, Harwell) for statistical analysis. This work was supported by the Department of Health, UK (Contract RRX95).

Table and Figure Legends

TABLE 1

^a LET and residual range values obtained for water using the computer program SRIM-2003 www.srim.org

^b For a cell with a measured average diameter of 7.9 μm

^c (see)

^d RBE for DNA dsb induction ~ 1 with the yield for low-LET radiation taken as 30 dsb per Gy

^e Estimated from , considering only complexity due to additional strand breaks. Inclusion of DNA base damage would further increase complexity.

^f range of δ -rays with maximum energy .

TABLE 3

To minimise the possibility of an over-prediction of complex size, only those complexes that were observed in cells that contained ‘no damage to homologous chromosome pairs’, were included. Therefore the total number of complexes shown in this Table is less than the number given in Table 2.

FIG. 1 (a). Schematic showing the relative range of the α -particles with respect to the average size of a CD34⁺ cell for the three energies used; (b) shows the variation in the LET across the cell as the α -particles slow down.

FIG. 2. Proportion of damaged cells that contain at least one simple or at least one complex exchange.

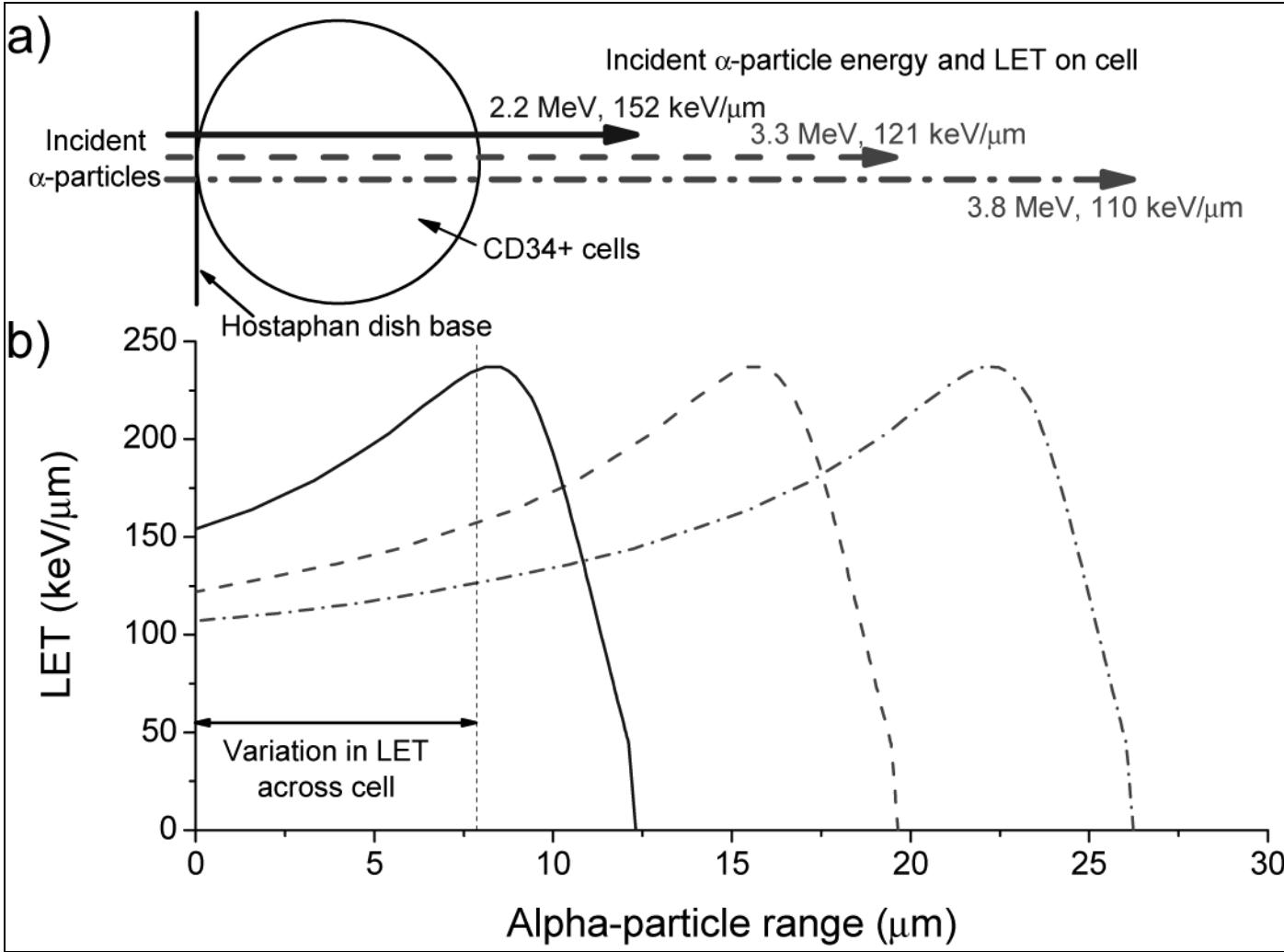
FIG. 3. Distribution of exchange aberrations in damaged cells. S (one simple exchange), S+ (simple_n+break_n), C (one complex exchange), C+ (complex_n+simple_n+break_n).

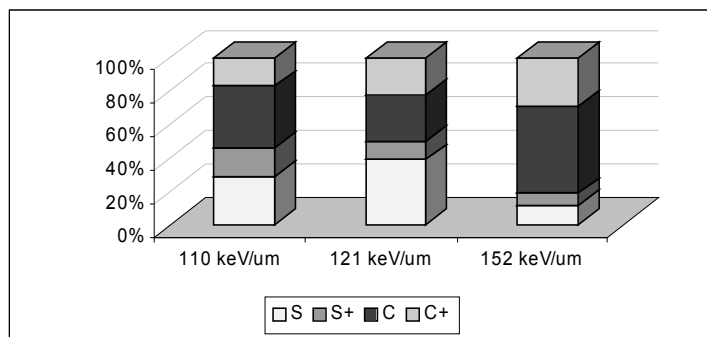
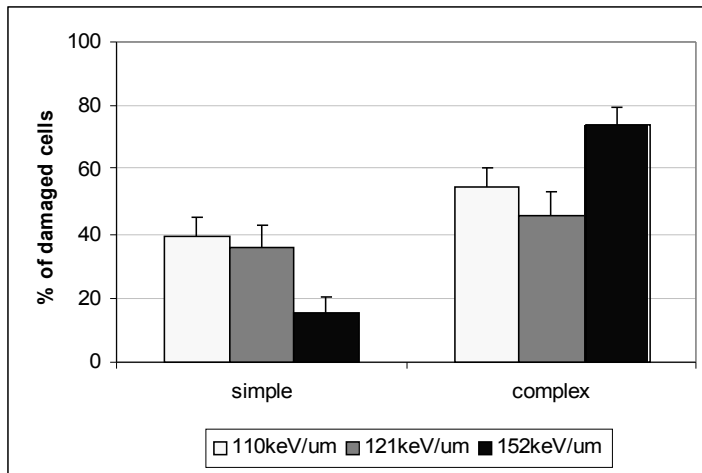
FIG. 4. Comparison between the number of independent events observed by m-FISH and the number of α -particle tracks per cell nucleus for each LET exposure. Observed data is expressed as a fraction of the total aberrant cells while the expected data is expressed as a fraction of traversed cells assuming a Poisson distribution.

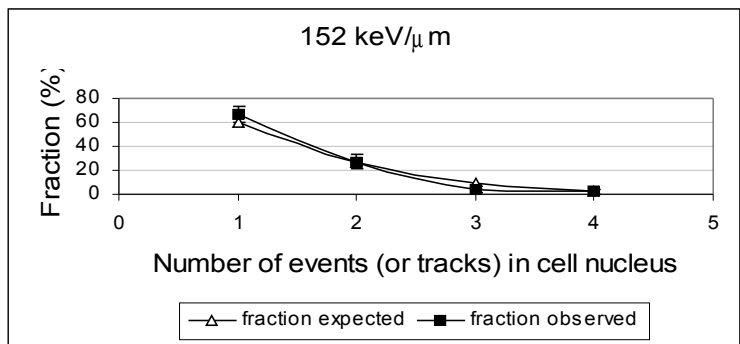
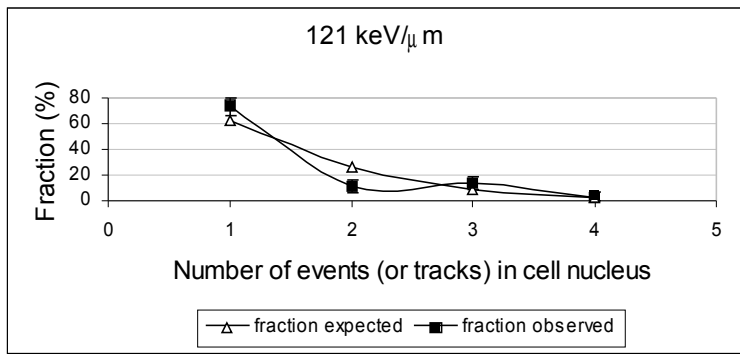
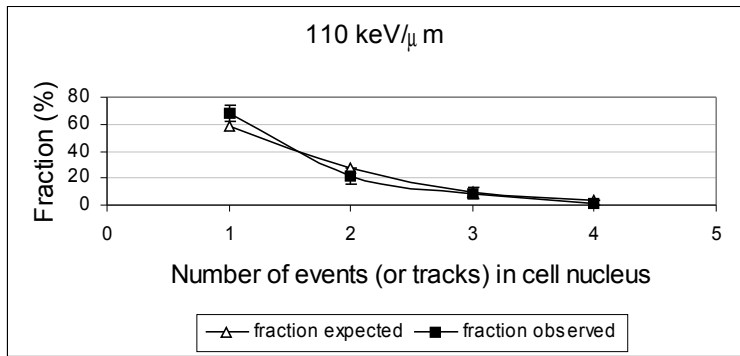
FIG. 5. Proportion of CD34⁺ cells in 1st, 2nd or 3rd cell division after exposure to α -particles of variable LET.

FIG. 6. Effect of LET of α -particle on the induction of apoptosis at varying times after exposure.

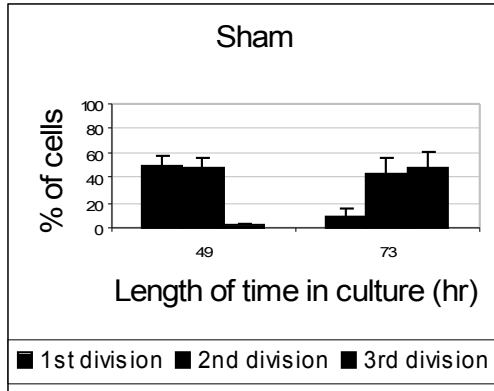
REFERENCES



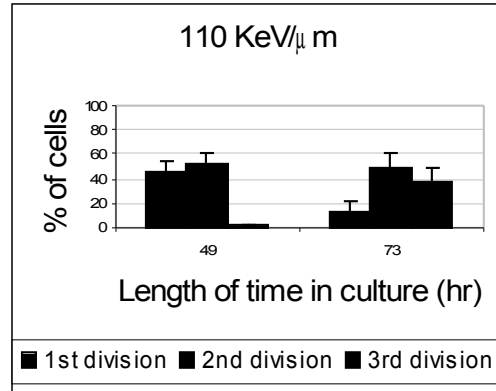




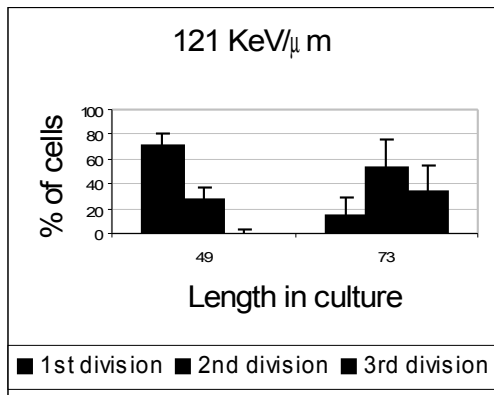
a



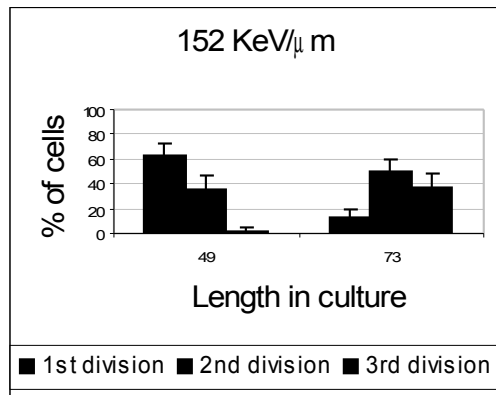
b



c



d



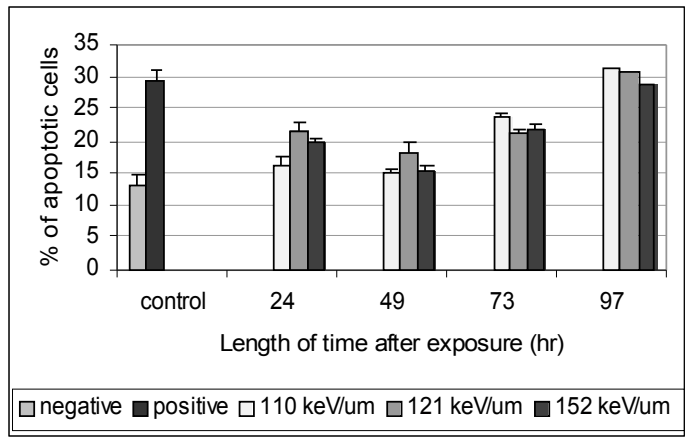


TABLE 1 α -particle exposure parameters and energy distribution in CD34⁺ cells

	α -particles		
LET ^a (keV/ μ m)			
Incident at cell base	110	121	152
Mean through cell ^b	119	135	182
Maximum ^b	131	153	220
Incident Energy ^c (MeV)	3.82	3.26	2.23
Range ^c (μ m)	25	20	13
Mean fluence ($\times 10^{-2} \mu\text{m}^{-2}$)	2.60	2.29	2.46
Entrance dose (Gy)	0.46	0.44	0.60
Mean dose through cell ^b (Gy)	0.50	0.49	0.71
Mean dose per traversal ^b (Gy)	0.39	0.44	0.60
Mean DNA dsb in cell per traversing track ^d	~12	~13	~18
% Complex double strand breaks ^e	60	64	73
δ -rays - maximum energy (keV)	2.1	1.8	1.2
- mean range ^f (μ m)	0.08	0.06	0.04

^a LET and residual range values obtained for water using the computer program SRIM-2003 www.srim.org

^b For a cell with a measured average diameter of 7.9 μ m

^c (see)

^d RBE for DNA dsb induction ~1 with the yield for low-LET radiation taken as 30 dsb per Gy

^e Estimated from , considering only complexity due to additional strand breaks. Inclusion of DNA base damage would further increase complexity.

^f range of δ -rays with maximum energy .

TABLE 2 Chromosome aberrations observed in CD34⁺ cells 49 hours after exposure and the calculated proportion of exchanges classified as complex.

Test	LET	Cells	% damaged	# Complex	# Simple	# Break	% complex
<u>Sham</u>		209	1	0	1 (0.005)	2 (0.01)	-
<u>~1 α-particle/cell</u>							
	110	213	30	39 (0.183)	49 (0.230)	13 (0.061)	44 %
	121	210	24	32 (0.152)	27 (0.129)	20 (0.095)	54 %
	152	254	23	52 (0.205)	24 (0.094)	13 (0.051)	68 %

TABLE 3 Total number and minimum size of complex aberrations in CD34⁺ cells after exposure to α -particles of various LET

Complex size		LET (keV/ μ m)		
Minimum number of:		110	121	152
Chromosomes	Breaks			
2	3	5	5	8
	4	1	1	2
	5	-	-	1
3	3	4	4	8
	4	4	3	5
	5	3	-	2
	6	1	-	-
4	8	-	-	1
	4	1	1	1
	5	3	3	1
	6	1	-	1
5	8	-	1	2
	6	1	2	-
	7	1	1	1
	8	-	2	-
6	10	1	-	-
	7	-	-	2
	8	1	-	-
7	11	1	-	-
	8	-	-	1
	9	1	-	-
8	11	-	-	1
	12	-	1	-

To minimise the possibility of an over-prediction of complex size, only those complexes that were observed in cells that contained ‘no damage to homologous chromosome pairs’, were included. Therefore the total number of complexes shown in this Table is less than the number given in Table 2.